

# Design and Analysis of Cavity Backed Spiral Antenna for Effective Antenna-Plasma Coupling in Tokamak Environments

Dimple Yadav<sup>a</sup>, Meenu Kaushik<sup>b</sup>, Raj Singh<sup>c</sup> & Vishant Gahlaut<sup>a,\*</sup>

<sup>a</sup>Department of Physical Sciences, Banasthali Vidyapith, Rajasthan 304 022, India

<sup>b</sup>School of Automation, Banasthali Vidyapith, Rajasthan 304 022, India

<sup>c</sup>RF and Fundamental Plasma Division, Institute for Plasma Research, Gandhinagar 382 428, India

Received: 31 July 2024; accepted: 22 May 2025

The study presents a novel approach to the designing and analyzing spiral antennas with cylindrical and conical-disc backings that are circularly polarized and optimized for antenna-plasma coupling in Tokamak settings. The intended frequency range for operation of the suggested antenna arrangement is 0.1 to 1.0 GHz. Unlike the traditional spiral antenna, which is supplied by a horizontally or vertically oriented balun, the proposed design is powered directly by a coaxial cable with a planar feeding section that has been specially calibrated to produce wide-band input impedance matching. The spiral antenna was designed with the steady state superconducting tokamak (SST-1) port area constraints in mind. With reflection coefficients of  $-24.05$  dB to feed conical backed cavities and  $-30.37$  dB to feed cylindrical backed cavities, respectively, the proposed antenna amply showed intrinsic resonance at 0.5GHz through modeling. The findings show encouraging progress in attaining efficient antenna-plasma interaction.

**Keywords:** SST-1, Antenna-Plasma coupling, Tokamak environments, Conical-disc, cylindrical backed, Spiral antenna

## 1 Introduction

In the pursuit of harnessing controlled nuclear fusion as a viable and sustainable energy source, Tokamak fusion reactors stand as prominent contenders. The intricate dynamics within the Tokamak plasma confinement chamber necessitate sophisticated electromagnetic systems, particularly antennas, to facilitate essential tasks such as diagnostics and control. One critical aspect of this electromagnetically challenging environment is the effective coupling between antennas and the plasma medium. A critical aspect of the design challenge for the required antenna solution is the development of a technique to ensure both impedance matching and bandwidth enhancement within a limited electrical size. Antennas with high gain and circular polarization are predominantly essential for the optimal performance of these wireless applications<sup>1</sup>. Belonging to the category of frequency-independent antennas, spiral antennas exhibit intrinsic circular polarization, along with a straightforward design, elevated gain, and wide-beam functionality<sup>2-3</sup>. These characteristics enable them to effectively meet the aforementioned requirements, making them a

preferred option for Tokamak environments. In recent times, the design of spiral antennas has become a focal point of interest for both academia and industry. Typically, these antennas are devised with a planar configuration that includes an Archimedean or logarithmic radiator, with possible shapes including circular, square, or rectangular<sup>2,4,5</sup>. To fulfill diverse specifications, researchers delve into different techniques and propositions for the efficient design of spiral antennas.

In a general classification, spiral antennas are divided into four distinct groups: spiral antennas operating in free space<sup>2,6,7</sup>, spiral antennas located on planar reflectors<sup>4,5,8</sup>, spiral antennas supported by cavities<sup>9,10</sup>, and spiral antennas installed on dielectric substrates<sup>11,12</sup>. In order to reduce the spiral antenna's size, a hybrid strategy that combines inductive as well as dielectric loading, along with a ground plane coated with ferrite, has been employed by Kramer *et al.*<sup>13</sup> Two FR-4 orthogonal dielectric slabs have been proposed by Kashyap *et al.* to improve the impedance spectrum of a dual-arm Archimedean spiral<sup>14</sup>. Afsar *et al.* have created a wide-band spiral antenna that consists of an inner turn Archimedean spiral and an outer turn Archimedean spiral having a zigzag design<sup>15</sup>. An Archimedean spiral antenna with

\*Corresponding author: E-mail: vgceeri@gmail.com

two arms composed of vertical metallic strips is proposed by Guraliuc *et al.* In this system, the strip width as well as turn thickness can be adjusted to precisely control the input impedance along with polarization purity<sup>16</sup>. A dual-band operational mode has been achieved by Chiu and Chuang *et al.* for the wide-band spiral antenna by integrating a frequency-selective surface (FSS) into its ground plane<sup>17</sup>. The ground plane serves as a reflective boundary, ensuring unidirectional radiation and supporting the cavity structure; thus, its conductivity directly affects the reflection coefficient and overall efficiency. Increased gain along with directivity is seen in spiral antennas supported by metallic reflectors or discs; however, Nakano *et al.*'s research<sup>4</sup> shows that this benefit is offset by a decrease in bandwidth. A design for a single-arm spiral antenna, incorporating a compact disc and supported by a cavity, has been proposed by Nakano *et al.* to enable ultra-wideband (UWB) operation<sup>18</sup>. According to Li *et al.*, the four-arm Archimedean helical antenna mounted on a metallic reflector as well as a contoured transmission line feed can be used to obtain a broad operational range of 0.8-3 GHz<sup>19</sup>. In order to accommodate the 868 MHz as well as 3.1-4.8 GHz frequency bands, Fantuzzi *et al.* have devised an innovative FR-4-based antenna configuration that combines a two-arm spiral with a meandering dipole<sup>20</sup>. Nakano *et al.* designed an equiangular spiral antenna to generate a unidirectional beam in the X-band frequency range, supported via an Electromagnetic Band Gap (EBG) reflector<sup>21</sup>. A new suggestion by Liu *et al.*<sup>22</sup> aims to increase bandwidth by introducing an Archimedean spiral featuring a hybrid structure that consists of a backed-cavity with an Electromagnetic Band Gap (EBG) along with a perfect electrical conductor. Liu *et al.* propose a hybrid form for the Archimedean spiral that combines a perfect electrical conductor and a backed cavity with an EBG to increase the bandwidth<sup>23</sup>. However, despite these advances, many existing spiral antenna designs face challenges in achieving compact form factors, wide impedance bandwidth, and effective plasma coupling—particularly in the electromagnetically harsh environment of a Tokamak reactor. In addition, maintaining circular polarization and high gain across a broad frequency range remains difficult when electrical size is constrained. These limitations underscore a clear need for a compact, low-profile spiral antenna that achieves efficient impedance matching and wide bandwidth while maintaining directional control and polarization purity.

This research addresses these challenges by proposing a novel spiral antenna design tailored specifically for antenna-plasma coupling in fusion reactor environments. This research introduces an investigative study that thoroughly examines a design approach for a compact and low-profile spiral antenna, specifically designed for antenna-plasma coupling impedance for operation in fusion reactors. The organization of this paper consists of four distinctive sections. Section II delves into a detailed account of the antenna design, elucidating the functioning of the innovative antenna through a comprehensive parametric study. Section III provides an analysis of the simulated results for the proposed antenna design. In Section IV encapsulates the findings, presenting the concluding remarks.

## 2 Innovative Approach in Antenna Design

### 2.1 Design Concept and Topology

Present spiral antenna is designed to fit and analyze it in the SST-1 tokamak. The opening port of SST-1 has a height of 280 mm, and if we take a diameter larger than this, there is a limiter installed on the back side of the space, so we cannot go beyond that diameter due to space constraints. Simplicity in geometry is a favored choice to alleviate complexity and the accompanying cost implications. To fulfill these criteria, a spiral structure is well-suited, owing to its inherent capability to provide wide bandwidth and circular polarization. The antenna delineated in this paper is a two arm conically backed cavity equiangular spiral antenna characterized by inherent resonance. Notably, it eschews external matching methodologies such as balun, stub tuners or phase shifter etc. a central transition section has been implemented, interfaced with a 50-ohm coaxial transmission line, facilitating autonomous impedance matching. To attain high gain and a unidirectional radiation pattern, the spiral is supported by a metallic disc, which is conically shaped to mitigate the tilt of the radiation pattern and enhance its symmetry around the bore sight. The gap between the spiral arms has been kept in such a way that there is no arching between those arms. Atmospheric pressure results in air breakdown at 30 kV/cm, breakdown will only occur if there is such an electric field, and a considerable voltage is required for such an electric field. However, in the actual case, there is no air inside the tokamak, and there is no atmospheric pressure, a very low pressure has been maintained.

Solving Maxwell's equations by using the Finite Integration Technique (FIT)<sup>24</sup>, the CST Microwave Studio software provides comprehensive analysis. Figure 1 illustrates the schematic layout of the modeled antenna structure, (a) Shows the perspective view of the design, (b) Shows the zoom in view of the feeding design, (c) Shows the top view of the conical backed cavity, and (d) Represents the top view of the cylindrical backed cavity. The design specifications for the suggested dual-arm spiral antenna to tokamak conditions are listed in Table 1.

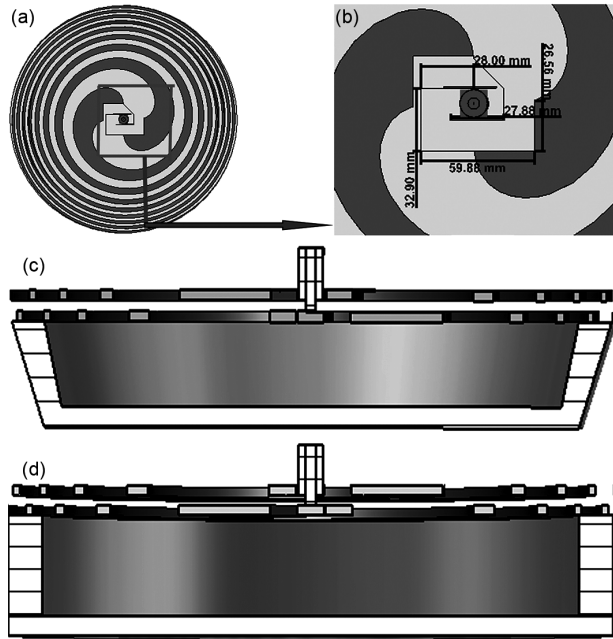


Fig. 1 — The design technique of cavity backed spiral antenna where, (a) the fronts view of the design, (b) the zoom view of the feeding section, (c) the top view of the conical cavity, and (d) the top view of cylindrical backed cavity

Table 1 — Optimized designed parameters for the proposed two-arm spiral antenna for tokamak environments

Antenna component	specifications	Dimensions (mm)
Cone-shaped disc	$h_c$	50
	$r_{c_{inner}}$	160
	$r_{c_{outer}}$	180
Cylindrical- shaped disc	$h_c$	50
	$r_{c_{inner}}$	160
	$r_{c_{outer}}$	180
Spiral	$n$	4
	$w_s$	8
	$h_s$	8
	$r_1$	140
	$r_0$	23.88
Coaxial transmission line	$C_{in}$	3
	$C_{out}$	7.25
	$L_c$	20

An equiangular spiral antenna is a type of logarithmic spiral antenna that radiates electromagnetic waves in a circularly symmetric pattern. The proposed antenna design leverages the unique properties of conical-disc backed spiral structures to enhance coupling with the plasma, thereby improving the overall performance of tokamak systems. The conical shape enhances the impedance bandwidth and radiation pattern, while the disc backing improves the antenna's impedance matching and radiation efficiency. The spiral structure is optimized for effective interaction with the tokamak plasma. The equation of equiangular spiral structure is represented as:

Assuming a structure is outlined in spherical coordinates as  $r = (\theta, \phi)$ , the excitation point resides at  $r = 0, \theta = 0, \phi = \pi$ . The self-scaling property of this structure becomes evident when a scaling factor  $K$  is applied [ $r' = K \cdot (\theta, \phi)$ ], resulting in an identical structure to  $r$ . In this scenario, the structure solely undergoes rotation around the  $\phi$  coordinate (Balanis, 2015), that is:

$$K \cdot F(\theta, \phi) = F(\theta, \phi + C) \quad \dots (1)$$

It is important to emphasize that  $C$ , being solely dependent on  $K$ , serves as the measure for the rotation angle of the diagram at frequency  $fk = f/k$ , relative to its position at frequency  $f$ . Obtaining  $(\theta, \phi)$  can be achieved by calculating the derivative of both sides of the equation with respect to  $C$  and  $\phi$ :

$$\frac{d}{dC} [K \cdot F(\theta, \phi)] = \frac{dK}{dC} [F(\theta, \phi)] = \frac{\partial}{\partial C} [F(\theta, \phi + C)] = \frac{\partial}{\partial(\phi+C)} [F(\theta, \phi + C)] \quad \dots (2)$$

$$\frac{d}{d\phi} [K \cdot F(\theta, \phi)] = K \cdot \left[ \frac{\partial F(\theta, \phi)}{\partial \phi} \right] = \frac{\partial}{\partial \phi} [F(\theta, \phi + C)] = \frac{\partial}{\partial(\phi+C)} [F(\theta, \phi + C)] \quad \dots (3)$$

By equalizing the last two terms, we obtain:

$$\frac{dK}{dC} [F(\theta, \phi)] = K \cdot \left[ \frac{\partial F(\theta, \phi)}{\partial \phi} \right] \quad \dots (4)$$

$$\frac{1}{K} \frac{dK}{dC} = \frac{1}{F(\theta, \phi)} \frac{\partial F(\theta, \phi)}{\partial \phi} = \frac{1}{r} \frac{\partial r}{\partial \phi} \triangleq a \quad \dots (5)$$

Ultimately, upon solving the partial differential equation, the resulting expression is:

$$r = e^{a\phi} f(\theta) \quad \dots (6)$$

Considering  $(\theta)$  as a function without specific constraints, this signifies the representation of an equiangular spiral on the surface described by  $(\theta)$ .

## 2.2 Parametric Study

An in-depth examination of structural parameters essential to antenna performance has been conducted to enhance the understanding of its operating principle. The analysis includes an examination of the impact of variations in spiral width ( $W_s$ ), cone height ( $h_c$ ), and substrate height ( $h_d$ ) on the  $S_{11}$ , -10 dB bandwidth, gain, of the proposed antenna. A parametric study of proposed conical backed equiangular spiral antenna is represented in Table 2 and for cylindrical backed equiangular spiral antenna is represented in Table 3.

In the elevated realm of the table, a parametric investigation has been conducted, wherein we systematically manipulated the outer radius of the spiral while holding constant the other parameters, including various conical and cylindrical heights. Through this comprehensive study, we have discerned that optimal outcomes are achieved when the outer radius is set at 140 mm and the conical height at 50 mm. In this configuration, we have ascertained a reflection coefficient of -24.05 dB, indicative of an exemplary impedance match. The voltage standing wave ratio (VSWR) stands at a commendable 1.58, and the gain attains a noteworthy value of 7.91 dBi.

A broader spiral arm yields an anticipated increase in gain; however, it concurrently diminishes bandwidth. Conversely, a slenderer spiral arm results in a reduction of gain and bandwidth. Altering the magnitude of this parameter markedly disrupts the antenna's impedance matching, inducing detuning as a consequence of perturbed current distribution along the spiral and a shift in the location of the current maxima. It is worth mentioning that while both parameters exert an influence, the impedance matching is significantly contingent on the outer radius of the spiral arm and, consequently, the air-gap. Consequently, the thoughtful selection of antenna dimensions is necessary to find equilibrium between the two parameters and elevate the antenna's performance to its zenith.

## 3 Results and Discussion

The antenna design is modified to comply with the port space constraints of SST-1, and then it is simulated with CST-MWS. The antenna exhibits intrinsic resonance at roughly 0.5GHz, featuring a reflection coefficient around -30.37 dB for a cylindrical cavity and -24.05 dB for a conical cavity, in accordance to the simulation results. In the radio

Table 2 — Parametric study of proposed conical backed equiangular spiral antenna

No. of turns	Conical height ( $h_c$ ) in mm	Spiral outer radius/ mm	Reflection coefficient $S_{11}$ [dB]	VSWR	Gain (dBic)
4	50	140	-24.05	1.58	7.91
		150	-7.70	9.38	7.81
		160	-1.71	8.16	7.13
	60	140	-12.51	1.63	7.94
		150	-22.30	1.16	7.89
		160	-12.77	1.59	6.69
6	50	140	-3.28	5.35	7.83
		150	-11.88	1.68	7.55
		160	-7.98	2.32	9.12
	60	140	-4.56	3.89	7.75
		150	-19.72	1.23	7.62
		160	-8.74	2.15	8.58

Table 3 — Parametric study of proposed cylindrical backed equiangular spiral antenna

No. of turns	Cylindrical height ( $h_c$ ) in mm	Spiral outer radius/ mm	Reflection coefficient $S_{11}$ [dB]	VSWR	Gain (dBic)
4	50	140	-28.01	1.10	7.98
		150	-8.01	2.33	8.071
		160	-1.81	9.60	7.76
	60	140	-12.90	1.77	7.85
		150	-11.73	1.70	7.93
		160	-2.15	8.09	7.73
6	50	140	-15.43	1.40	8.08
		150	-8.28	2.25	7.89
		160	-17.27	1.31	7.71
	60	140	-11.08	1.77	7.85
		150	-12.60	1.61	7.93
		160	-10.76	1.81	7.73

frequency range, the antenna prototype has a directional radiation pattern has broadside gain values more than 5 dBic for both cavity-backed constructions. In order to facilitate coaxial feeding for both arms, an optical waveguide port is positioned at the center of the spiral. The next section displays the calculated S-parameters of the recommended antenna array expressed in terms of the reflection coefficient. Other crucial characteristics like radiation pattern along with impedance are examined and discussed in the subsection that follows.

**3.1 Reflection Coefficient**

According to Fig. 2, the antenna registers its reflection coefficient about -24.05 dB to conical backed cavities as well as -30.37 dB to cylindrical backed cavities, indicating that it perfectly satisfies optimal impedance matching at the designated 500-megahertz frequency. This number indicates that the majority of the signal power is either conveyed as well absorbed by the system, with very little of it being reflected back. This comparatively little amount of reflection shows efficient energy transfer.

**3.2 Voltage Standing Wave Ratio (VSWR)**

Figure 3 illustrates a near-perfect impedance coherence within the antenna as well as the transmission line at 500-megahertz frequency, where the antenna displays a VSWR frequency close to (VSWR>2). A VSWR value that is near to 1 indicates low signal reflection along with efficient power transfer. This indicates that the framework is optimized for signal integrity and minimizes losses resulting from mismatched signals.

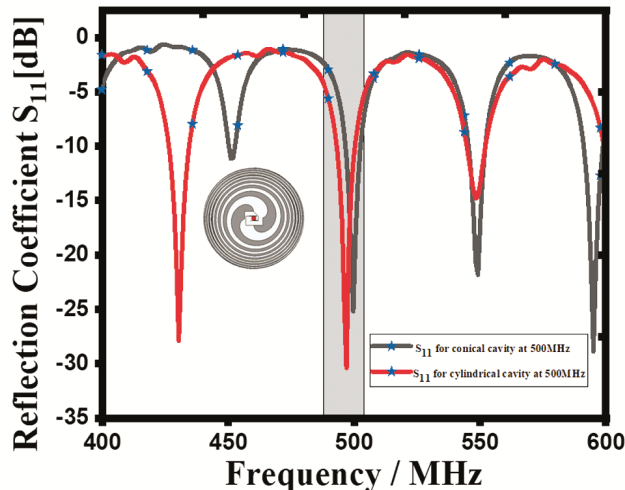


Fig. 2 —  $S_{11}$  of cavity backed equiangular spiral antenna

**3.3 Z-Matrix**

When powered via a 50  $\Omega$  coaxial transmission line, the z-matrix describes its impedance characteristics. In this instance, the antenna's input impedance shows an opposing resistance of 60.13 $\Omega$  as well as a reactance of -3.94 $\Omega$ , with a conical backed cavity that has a real part of 60.13 as well as an unreal part of -3.94. Figure 4 illustrates the input impedance associated with the antenna, which shows a resistance of 55.35 $\Omega$  as well as a reactance of -2.06 $\Omega$  within the cylindrical backed cavity, whereas the actual portion is 55.35 while the imaginary part is -2.06. This implies that there is adequate impedance matching and effective flow of energy in the middle of the transmission line as well as the antenna because the antenna's impedance nearly matches the 50 $\Omega$  feed.

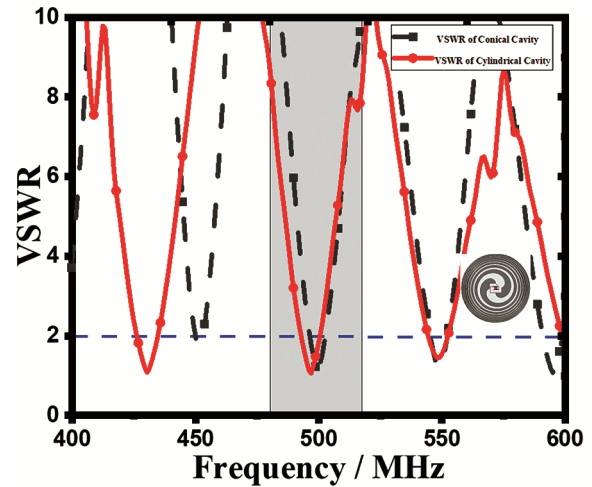


Fig. 3 — VSWR of cavity backed equiangular spiral antenna

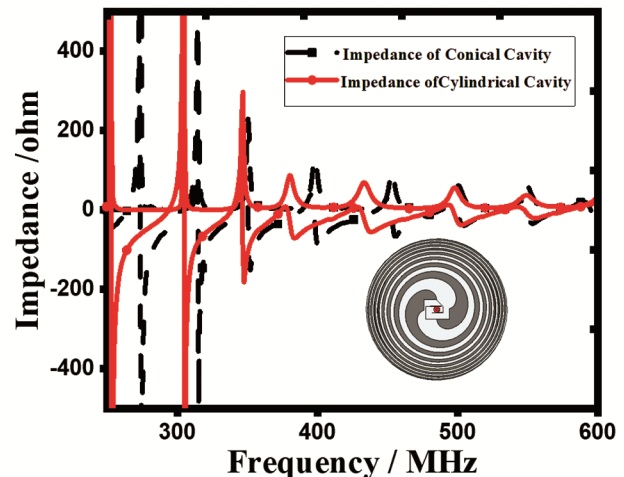


Fig. 4 — Z-matrix of cavity backed equiangular spiral antenna

**3.4 Gain**

A gain of 7.91 dBi of conical backed cavity and 7.48 dBi of cylindrical backed cavity at 500MHz (shown in Fig. 5) implies that electromagnetic energy is effectively radiated in the specified direction by antennas. At situations where concentrated electromagnetic energy is required, this gain level is a good indication of the antenna's directional ability, which can improve signal transmission as well reception.

**3.5 Radiation and Total Efficiency**

An antenna's ability to convert input power into electromagnetic energy that is then emitted is evaluated by its radiation efficiency. Nearly all of the input power is transformed into useful radiated energy at 500 megahertz (Fig. 6), as indicated by the conical

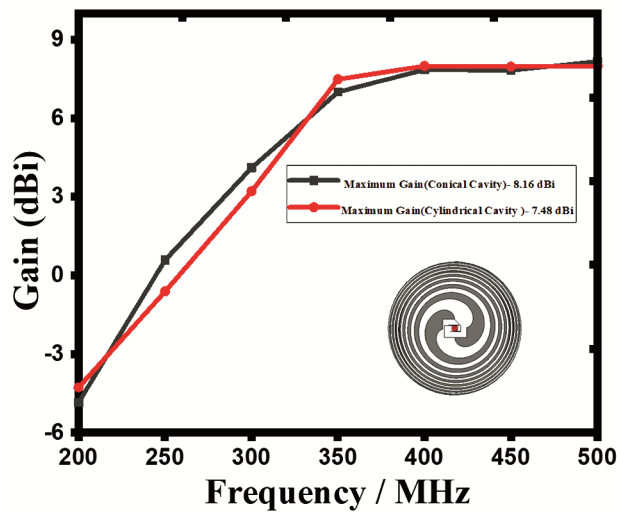


Fig. 5 — Gain of cavity backed equiangular spiral antenna

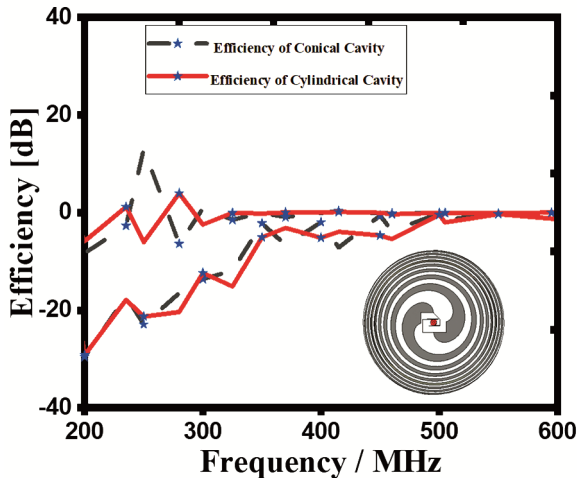


Fig. 6 — Efficiency of cavity backed equiangular spiral antenna

backed cavity as well as the cylindrical backed cavity with equiangular spiral antenna representing the radiation efficiency more than 90%. This implies that the antenna transmits signals effectively and with little loss of signal transmission power.

**3.6 Surface Current Distribution**

It refers to how electric charge transport is arranged spatially along the boundaries among conductive as well as dielectric materials when electromagnetic fields are present. In high-temperature tokamak environments, these materials must exhibit excellent thermal stability, high electrical conductivity, and resistance to radiation damage. For both the conical-disc and cylindrical-backed cavities, materials such as oxygen-free high-conductivity (OFHC) copper or silver-plated aluminum are typically preferred due to their low surface resistance and effective RF performance. The maximum electric current density often builds up at the center coaxial feeding mechanism. This phenomenon improves impedance matching, radiation properties, along with antenna reliability. Figure 7(a-b) represents the current distribution of conical and cylindrical backed spiral antenna.

**3.7 Radiation Pattern**

Graphs known as radiation patterns display the many directions in which electromagnetic energy is transmitted into space by an antenna as well other

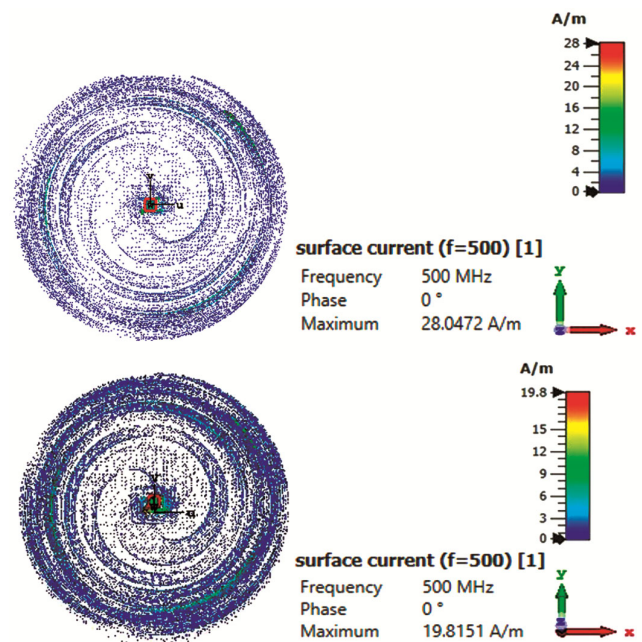


Fig. 7 — (a) Current distribution of cavity backed equiangular spiral antenna and (b) Surface current distribution of cavity backed equiangular spiral antenna

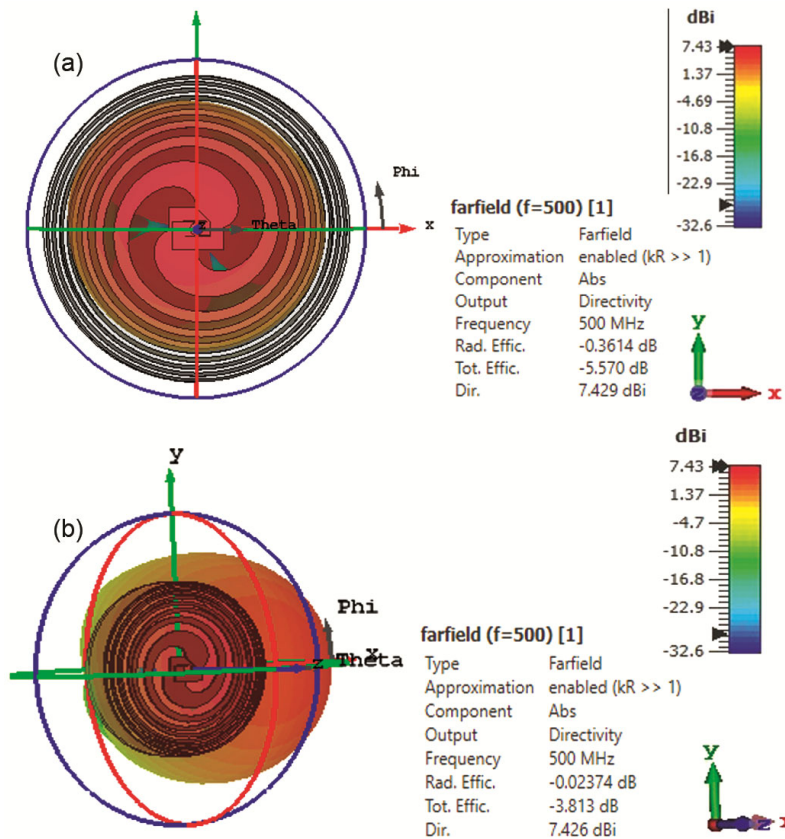


Fig. 8 — (a) 3D graph of the cavity backed equiangular spiral antenna and (b) 3D graph of the cavity backed equiangular spiral antenna

Table 4 — Result of the proposed cavity backed equiangular Spiral Antenna

Antenna Profile	Compact size and simple (Conical cavity)	Compact size and simple (Cylindrical cavity)
Operating Bandwidth	14 % (~480 to ~550 MHz)	16 % (~450 to ~530 MHz)
Reflection Coefficient	-24.05 dB	-30.37 dB
VSWR	1.18	1.06
Efficiency	High (> 90%)	High (> 90%)
Impedance Matching	Z <sub>1,1</sub> (Re)= 60.13 Z <sub>1,1</sub> (Im)= -3.94	Z <sub>1,1</sub> (Re)= 55.35 Z <sub>1,1</sub> (Im)= -2.06
Radiation Pattern	unidirectional	unidirectional
Gain	7.91 dBi	7.48 dBi

electromagnetic device. Figure 8(a-b) show the 3D radiation characteristics at 500 MHz for the given antenna in the cases of conical and cylindrical cavities, respectively. The radiation pattern of the envisaged spiral antenna is unidirectional.

**4 Conclusion**

The study design and analysis of conical-disc backed and cylindrical backed equiangular spiral antennas offers a proper solution to the problems of antenna-plasma coupling in tokamak environments. By improving the effectiveness of plasma heating and diagnostics in tokamak operations, the suggested antenna design hopes to further the study of magnetic

confinement fusion. A thorough comparison of the coupling impedance between a conical-backed cavity and a cylindrical-backed cavity has been carried out. An excellent impedance match is shown by the obtained reflection coefficients of -24.05 dB for the conical cavity and -30.37 dB for the cylindrical cavity. The antenna's ability to efficiently boost signal strength is demonstrated by the obtained gains of 7.91 dBi and 7.48 dBi, which support dependable and durable communication. It is clear from Table 4 above that the results from the cylindrical cavity are superior than those from the conical one. The antenna's applicability in plasma coupling settings is demonstrated by its impressive efficiency of over

90%, which was achieved using CST-MWS. Furthermore, the impedance matching capabilities that have been proven highlight how adaptable it is to changing plasma circumstances.

## References

- 1 Ur-Rehman M, Safdar G A, Yang X & Chen X, *IEEE Access*, 5 (2017) 21344.
- 2 Curtis W, *IRE Trans Antennas Propag*, 8 (3) (1960) 298.
- 3 Dyson J, *IRE Trans Antennas Propag*, 7 (2) (1959) 181.
- 4 Nakano H, Nogami K, Arai S, Mimaki H & Yamauchi J, *IEEE Trans Antennas Propag*, 34 (6) (1986) 791.
- 5 Wang J J & Tripp V K, *IEEE Trans Antennas Propag*, 39 (3) (1991) 332.
- 6 Kaiser J (1960), *IRE Trans Antennas Propag*, 8 (3) (1960) 312.
- 7 Gloutak R T & Alexopoulos N G, *IEEE Trans Antennas Propag*, 45 (4) (1997) 723.
- 8 Ur-Rehman M, Abbasi Q H, Kamran M & Yang X, In *2013 IEEE International RF and Microwave Conference (RFM)*, 2013, 318.
- 9 Kramer B A, Lee M, Chen C C & Volakis J L, *IEEE Trans Antennas Propag*, 53 (7) (2005) 2193.
- 10 Rahman N & Afsar M N, *IEEE Trans Antennas Propag*, 61 (1) (2012) 54.
- 11 Nakano H, Ikeda M, Hitosugi K & Yamauchi J, *IEEE Trans Antennas Propag*, 52 (6) (2004) 1417.
- 12 Penney C W & Luebbbers R J, *IEEE Trans Antennas Propag*, 42 (9) (1994) 1328.
- 13 Kramer B A, Chen C C & Volakis J L, *IEEE Antennas Wireless Propag Letters*, 7 (2008) 22.
- 14 Kashyap N & Vishwakarma D K, *IEEE Antennas Wireless Propag Letters*, 15 (2015) 589.
- 15 Afsar M N, Wang Y & Cheung R, *IEEE Antennas Propag Magazine*, 46 (1) (2004) 59.
- 16 Guraliuc A R, Caso R, Nepa P & Volakis J L, *IEEE Antennas Wireless Propag Letters*, 11 (2012) 168.
- 17 Chiu C N & Chuang W H, *IEEE Antennas Wireless Propag Letters*, 8 (2009) 624.
- 18 Nakano H, Satake R & Yamauchi J, *IEEE Trans Antennas Propag*, 58 (5) (2010) 1511.
- 19 Li D, Li L, Li Z & Ou G, *IEEE Antennas Wireless Propag Letters*, 16 (2016) 62.
- 20 Fantuzzi M, Masotti D & Costanzo A, *IEEE Trans Antennas Propag*, 63 (9) (2015) 3839.
- 21 Nakano H, Kikkawa K, Kondo N, Iitsuka Y & Yamauchi J, *IEEE Trans Antennas Propag*, 57 (5) (2009) 1309.
- 22 Liu C, Lu Y, Du C, Cui J & Shen X, *IEEE Trans Antennas Propag*, 58 (6) (2010) 1876.
- 23 Liu P, Yang S, Wang X, Yang M, Song J & Dong L, *IEEE Antennas Wireless Propag Letters*, 16 (2016) 66.
- 24 Studio C M, *CST Studio Suite*, (2024).